

# Superconductivity at 38 K in an electrochemical interface between ionic liquid and Fe(Se<sub>0.8</sub>Te<sub>0.2</sub>) on various substrates

Shunsuke Kouno,<sup>1</sup> Yohei Sato,<sup>1</sup> Yumiko Katayama,<sup>1</sup> Ataru Ichinose,<sup>2</sup> Daisuke Asami,<sup>1</sup> Fuyuki Nabeshima,<sup>1</sup> Yoshinori Imai,<sup>3</sup> Atsutaka Maeda,<sup>1</sup> and Kazunori Ueno<sup>1\*</sup>

<sup>1</sup>*Department of Basic Science, University of Tokyo, Meguro, Tokyo 115-8902, Japan*

<sup>2</sup>*Central Research Institute of Electric Power Industry, Yokosuka, Kanagawa 240-0196, Japan*

<sup>3</sup>*Department of Physics, Tohoku University, Sendai 980-8578, Japan*

\*Correspondence to: ueno@phys.c.u-tokyo.ac.jp

## ABSTRACT

Superconducting FeSe<sub>0.8</sub>Te<sub>0.2</sub> thin films on SrTiO<sub>3</sub>, LaAlO<sub>3</sub> and CaF<sub>2</sub> substrates were electrochemically etched in an ionic liquid DEME-TFSI electrolyte with a gate bias of 5 V. Superconductivity at 38 K was commonly observed on all substrates after etching the films with a thickness above 30 nm, in spite of different  $T_c$  of 8 K, 12 K and 19 K before the etching on SrTiO<sub>3</sub>, LaAlO<sub>3</sub> and CaF<sub>2</sub> substrates, respectively.  $T_c$  returned to the original value by removing the gate bias. The  $T_c$  enhancement on the thick film indicates no relationship between the  $T_c$  enhancement and any interface effects between the film and the substrate. The sheet resistance and the Hall coefficient of the surface conducting layer were estimated from the gate bias dependence of the transport properties. The sheet resistance of the surface conducting layer of the films on LaAlO<sub>3</sub> and CaF<sub>2</sub> showed an identical temperature dependence, and the Hall coefficient is almost temperature independent and -0.05 to -0.2 m<sup>2</sup>/C, corresponding to 4-17 electrons per one FeSe<sub>0.8</sub>Te<sub>0.2</sub> unit cell area in two dimension. These common transport properties on various substrates suggest that the superconductivity at 38 K appeared in the surface conducting layer produced by electrochemical reaction between the surface of the FeSe<sub>0.8</sub>Te<sub>0.2</sub> thin film and the ionic liquid electrolyte.

FeSe is an iron-based superconductor with the most simple composition and exhibits superconductivity at 8.5 K.<sup>1</sup> FeSe recently attracts much attention owing to an enhancement in superconducting transition temperature ( $T_c$ ) by various method.  $T_c$  in one-unit-cell FeSe thin film on a SrTiO<sub>3</sub> substrate was reported to be 105 K and 85 K by an in-situ resistivity measurement and a diamagnetic measurement, respectively.<sup>2,3</sup> Spectroscopic study on monolayer or several-layers FeSe on SrTiO<sub>3</sub> showed that a superconducting gap corresponding to 65 K and 80 K by ARPES and STM, respectively.<sup>4-6</sup> These values are much higher than the bulk  $T_c$  of all known iron-based superconductors.  $T_c$  of 48 K was also observed in a several-layers FeSe on SrTiO<sub>3</sub> with a carrier doping by K ions.<sup>7</sup> The  $T_c$  enhancement has been considered to originate from a charge transfer from the oxide substrate to FeSe ultrathin film.<sup>6</sup>  $T_c$  enhancement up to around 40 K has also been reported by insertion of cations or (Li<sub>0.8</sub>Fe<sub>0.2</sub>)OH layer to FeSe mother compound.<sup>8-14</sup> Recently, electrostatic carrier doping on ultrathin FeSe films and a flake also enhanced  $T_c$  up to around 40 K.<sup>15-19</sup> They employed an electric double layer transistor (EDLT) configuration with an ionic liquid DEME-TFSI as a gate electrolyte for tuning high density carriers.<sup>20-22</sup> Since no extra-phase except for FeSe was found in XRD data,<sup>18</sup> the  $T_c$  enhancement is considered to originate from electrostatic carrier doping. In addition, thickness dependence study by an electrochemical etching of FeSe showed that  $T_c$  enhancement only occurred when the film is thinner than 15 nm,<sup>16,19</sup> probably indicating that the interface between the film and the substrate also plays an important role to the  $T_c$  enhancement.

We have reported on a  $T_c$  enhancement in FeSe<sub>1-x</sub>Te<sub>x</sub> thin films on various substrates.<sup>23-26</sup> In addition, the  $T_c$  depends both on Te content and substrate materials. For example,  $T_c$  for FeSe<sub>0.8</sub>Te<sub>0.2</sub> films on CaF<sub>2</sub> and LaAlO<sub>3</sub> substrates are enhanced to 20 K and 12 K, respectively, contrasting to  $T_c$  of 8 K for FeSe<sub>0.8</sub>Te<sub>0.2</sub> on SrTiO<sub>3</sub>. This was explained by a change of a-axis lattice constant of the FeSe<sub>0.8</sub>Te<sub>0.2</sub> films on various substrates.<sup>24</sup> In this study, we report on the  $T_c$  enhancement of thick Fe(Se<sub>0.8</sub>Te<sub>0.2</sub>) films on various substrates up to 38 K by the EDLT fabrication with ionic liquid DEME-TFSI. By using the electrochemical etching technique with the ionic liquid,<sup>16</sup> the thickness of the film was varied. An application of the gate bias formed a surface conducting layer with  $T_c$  of 38 K, and by removing the gate bias, the surface conducting layer disappeared and  $T_c$  returned to the original value. We also estimated transport properties of the surface conducting layer. The surface conducting layer showed an electron conduction with a common temperature dependence of mobility on various substrates.

Fe(Se<sub>0.8</sub>Te<sub>0.2</sub>) thin films were deposited by a PLD method with a KrF excimer laser with a Fe(Se<sub>0.8</sub>Te<sub>0.2</sub>) polycrystalline target. Detailed fabrication conditions are described elsewhere.<sup>27,28</sup> We used commercially available SrTiO<sub>3</sub> (001) (STO) substrate with step-and-terrace surface, LaAlO<sub>3</sub> (001) (LAO) substrate and CaF<sub>2</sub> (001) substrate. AFM and X-ray diffraction measurements were

carried out prior to the device fabrication. Au(100 nm) / Ti (20 nm) films were electron-beam evaporated with a base pressure of  $10^{-5}$  Torr. Since  $\text{Fe}(\text{Se}_{0.8}\text{Te}_{0.2})$  thin films are damaged by high temperature above 100 deg.C and water during the standard photolithography and the dry etching process, we employed a sand-blast technique at room temperature for the fabrication of a Hall-bar. The films were coated by a dry film resist patterned by photolithography, and etched by a sand-blast with alumina emery (#220). As shown in Fig. 1(a), an EDLT device has six-terminal Hall-bar shaped electrodes and Pt film worked as a gate electrode placed aside the Hall-bar sample. The Hall-bar electrodes and wirings were coated by a silicone sealant to prevent electrochemical reaction between an electrolyte and the Au/Ti electrode. Ionic liquid DEME-TFSI was dipped on a channel area of the Hall-bar and the Pt film. Electrochemical etching and transport measurements were carried out in He atmosphere by Quantum Design PPMS at temperature from 300 K to 2 K.

The film thickness and crystal quality were examined by XRD measurements. Figure 1 (a) shows XRD patterns for  $\text{FeSe}_{0.8}\text{Te}_{0.2}$  thin films fabricated on LAO,  $\text{CaF}_2$  and STO substrates. All samples showed (001), (002) and (004) peaks, while (003) peak for the film on LAO substrate was overwrapped with a (002) peak of the substrate. A c-axis lattice constants for the films on LAO,  $\text{CaF}_2$  and STO substrates are 5.69, 5.72 and 5.70 Å, respectively, which are consistent with previous reports.<sup>23,24</sup> FWHM of the rocking curve for the (001) peak were 0.4, 0.7 and 1 deg. for the films on LAO,  $\text{CaF}_2$  and STO substrates, respectively, which is also almost same as those in the previous report (0.2-0.6 deg.)<sup>23</sup>, demonstrating that all of these films are of high quality single-phased samples. X-ray reflectivity (XRR) measurements show clear thickness fringes for all films, as shown in Fig. 1 (b), indicating smooth surface and sharp interface between the film and the substrate. In addition, all XRR curves were well fitted by the model structure, and we estimated the thickness as shown in Fig. 1(b). The film thickness was also confirmed by AFM images for the films.

-Figure 1

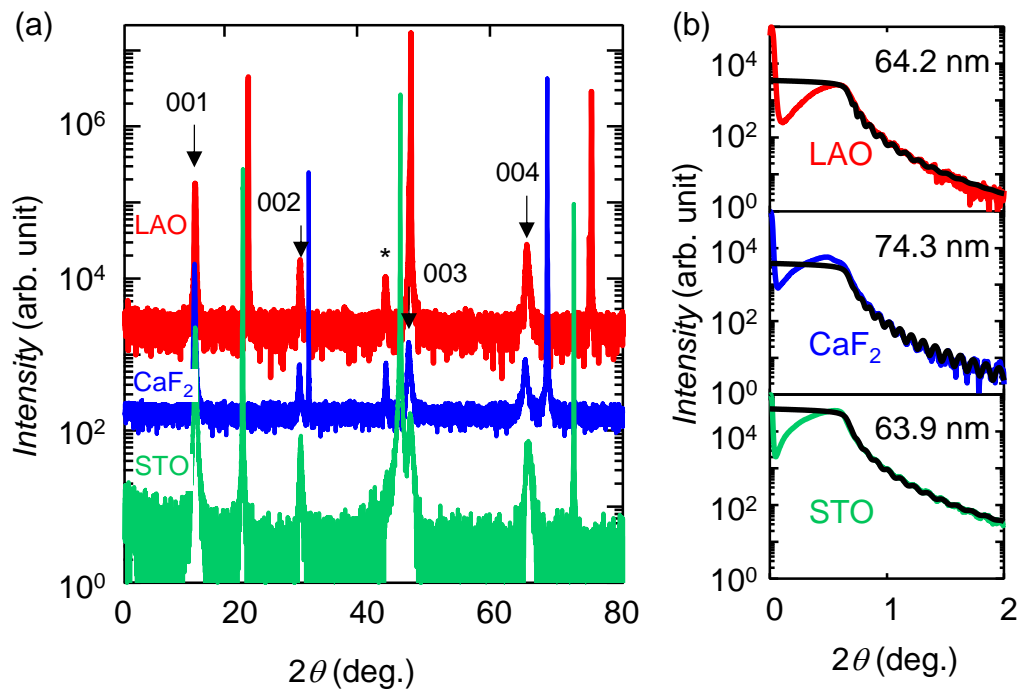


Figure 1 (a) XRD diffraction patterns for FeSe<sub>0.8</sub>Te<sub>0.2</sub> thin films on LaAlO<sub>3</sub> (LAO), CaF<sub>2</sub> and SrTiO<sub>3</sub> (STO) substrates. (b) X-ray reflectivity (XRR) patterns for the films. Black lines show fitting curves. Estimated thicknesses are shown in each panel.

Superconducting properties were examined with gating and etching for the gate bias ( $V_G$ ) of 5 V. Figures 2 (c) and (d) show temperature ( $T$ ) dependence of the sheet resistance ( $R_S$ ) for samples on Fe( $\text{Se}_{0.8}\text{Te}_{0.2}$ ) films on LAO and  $\text{CaF}_2$  substrates (LAO and  $\text{CaF}_2$  samples), respectively. First, the  $R_S$ - $T$  curves were measured for  $V_G$  of 0 V and 5 V for the pristine device before etching. Then, the temperature was increased to 250 K with  $V_G$  of 5 V with monitoring the gate current ( $I_G$ ), as shown in Fig. 2 (b). The channel of the device was electrochemically etched and the drain current ( $I_D$ ) was gradually decreased. A product of  $I_G$  and the time is a Faradaic charge ( $Q_F$ ), which is proportional to an amount of charges of reacted ions. After the etching,  $T$  was decreased for  $V_G = 5$  V, and the  $R_S$ - $T$  curve was measured. After several cycles of the etching,  $V_G$  dependence of  $R_S$ - $T$  curve for the etched device was measured by following procedure: first, the  $R_S$ - $T$  curve was measured for 5 V. Then, the temperature was increased to 250 K without  $V_G$ , and the  $R_S$ - $T$  curve for  $V_G = 0$  V was measured. Finally,  $V_G$  of 5 V was applied at 250 K, and the  $R_S$ - $T$  curve for  $V_G = 5$  V was measured again. We showed the  $R$ - $T$  curves for the pristine device, and those for the etched device for  $V_G = 5$  V,  $V_G = 0$  V, and  $V_G = 5$  V. The  $R_S$ - $T$  curves for the pristine sample was almost unchanged between  $V_G$ s of 0 V and 5 V. In contrast,  $T_c$  was enhanced by several cycles of etching for  $V_G = 5$  V.  $T_c$  changed from 12 K to 38 K for the LAO sample, and 19 K to 38 K for the  $\text{CaF}_2$  sample. By removing  $V_G$ ,  $R_S$  increased and  $T_c$  was returned to the value of the pristine sample. By applying  $V_G$  of 5 V,  $R_S$  slightly decreased and  $T_c$  was also enhances to 38 K for both samples. It is noted that  $R_S$  for  $V_G = 5$  V after removing  $V_G$  is smaller than that before removing  $V_G$ . Since sheet resistance should have an identical value with  $V_G = 5$  V by the electrostatic carrier doping, this change suggests that there is another origin of a change in  $R_S$  than the electrostatic carrier doping. This will be discussed later. Figures 2 (e) and (f) show the  $T$  dependence of Hall coefficient ( $R_H$ ) for the same devices shown in Figs. 2 (c) and (d), respectively.  $R_H$  was almost zero above 80 K and showed increase with decreasing temperature below 40 K for the pristine sample. In contrast,  $R_H$  was always negative at all temperatures for the etched sample for  $V_G$  of 5 V.  $R_H$ - $T$  behavior returned to almost the original one after applying  $V_G$  of 0 V. Those results indicate that the etching for  $V_G$  of 5 V formed a conducting layer on a surface with  $T_c$  of 38 K for both the LAO and  $\text{CaF}_2$  sample. Since  $R_H$  was negative, an electron conduction dominates in the conductive layer. In addition, since the transport properties of the pristine device and the etched device for  $V_G$  of 0 V was almost the same, the surface conductive layer disappeared by removing  $V_G$  for the etched sample.

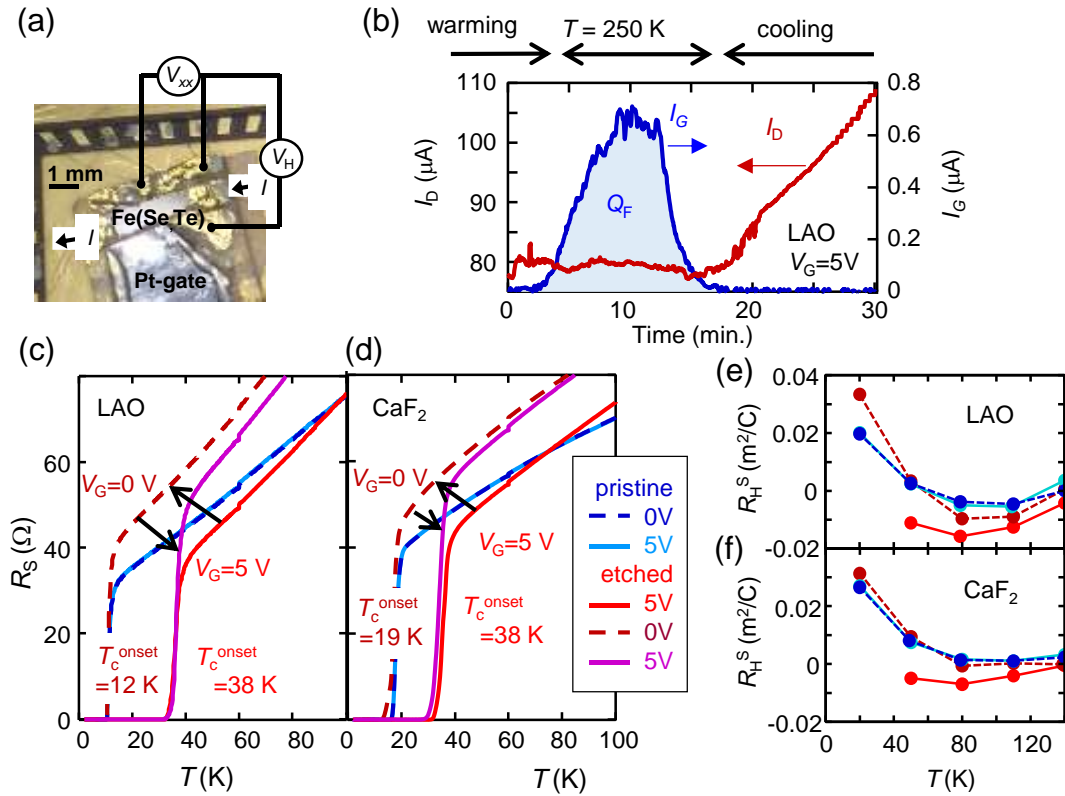


Figure 2 (a) Photographic image for the EDLT device on the  $\text{FeSe}_{0.8}\text{Te}_{0.2}$  / LAO sample. Four-terminal resistance and Hall resistance are simultaneously measured with the Hall-bar shaped electrodes. Ionic liquid electrolyte is placed between the film and the Pt gate. (b) Time dependence of the drain current ( $I_D$ ) and the gate current ( $I_G$ ) during the electrochemical etching for  $V_G = 5$  V at 250 K for the  $\text{FeSe}_{0.8}\text{Te}_{0.2}$  /LAO sample.  $I_G$  corresponds to the Faradaic current, and the product of  $I_G$  and the time corresponds to the Faradaic charge ( $Q_F$ ). (c), (d) The temperature ( $T$ ) dependence of sheet resistance ( $R_S$ ) for a pristine sample (blue) and an etched sample (red). Data for  $V_G = 0$  V and 5 V are shown by broken and solid lines, respectively. The etched sample was measured for  $V_G = 5$  V (red),  $V_G = 0$  V (broken red), and then  $V_G = 5$  V (purple). The samples were fabricated on (c) LAO and (d)  $\text{CaF}_2$  substrates. (e),(f) The  $T$  dependences of Hall coefficient ( $R_H$ ) for the pristine and the etched samples for  $V_G$  of 0 V and 5 V for samples fabricated on LAO and  $\text{CaF}_2$  substrates, respectively.

Thickness dependence of the superconducting properties was also examined for the LAO, CaF<sub>2</sub> and STO samples. Figures 3 (a), (b), and (c) show the  $R_S$ - $T$  curves for the LAO, CaF<sub>2</sub> and STO samples with various thickness (etching cycles), respectively.  $R_S$  was normalized by  $R_S$  at 100 K. For the LAO and CaF<sub>2</sub> samples,  $T_c$  was enhanced after several cycles of the etching. The CaF<sub>2</sub> sample showed a two-step superconducting transition at the initial stage of the etching. Similar two-step transition has been reported on the EDLT on the FeSe flake with a gate bias of around 4 V, ascribed to an inhomogeneity of the carrier distribution.<sup>15</sup> In addition, the normalized  $R_S$ - $T$  curves are almost identical after the  $T_c$  enhancement. In contrast, for the STO sample,  $T_c$  gradually enhanced from 8 K to 38 K with many cycles. We estimated an onset temperature ( $T_c^{\text{onset}}$ ) of superconductivity from the  $R_S$ - $T$  curve as shown in Fig. 3(a). We also estimated the thickness after  $n$  cycles of etching,  $thickness(n)$ , from an equation,

$$thickness(n) = thickness(XRR) \times \sum_{i=1}^n Q_F / \sum_{i=1}^{n_{\text{total}}} Q_F,$$

where  $Q_F$  is the Faradaic charge for each cycle,  $thickness(XRR)$  is the film thickness before the etching estimated from the XRR measurement, and  $n_{\text{total}}$  is the total cycles needed for the etching of the entire film. Figure 3 (d) shows the thickness dependence of  $T_c^{\text{onset}}$  for the LAO, CaF<sub>2</sub> and STO samples.  $T_c$  started to increase only after two cycles of the etching and saturated at 38 K after four cycles for the LAO and CaF<sub>2</sub> samples. As shown in the previous paragraph,  $T_c$  decreased to the original value by removing  $V_G$  at 250 K, but  $T_c$  returned to 38 K after the next cycle for  $V_G = 5$  V. The STO sample showed the  $T_c$  enhancement from 8 K to 16 K at the thickness of 30 nm, and  $T_c$  enhancement to 38 K at the thickness of 10 nm. Since the  $T_c$  enhancement occurred in thick samples on all substrates, and since  $T_c$  changed by applying and removing  $V_G$ , we concluded that the  $T_c$  enhancement is not affected by the interface between the substrate and the film, but originates from the surface conducting layer produced by  $V_G = 5$  V.

Figure 3

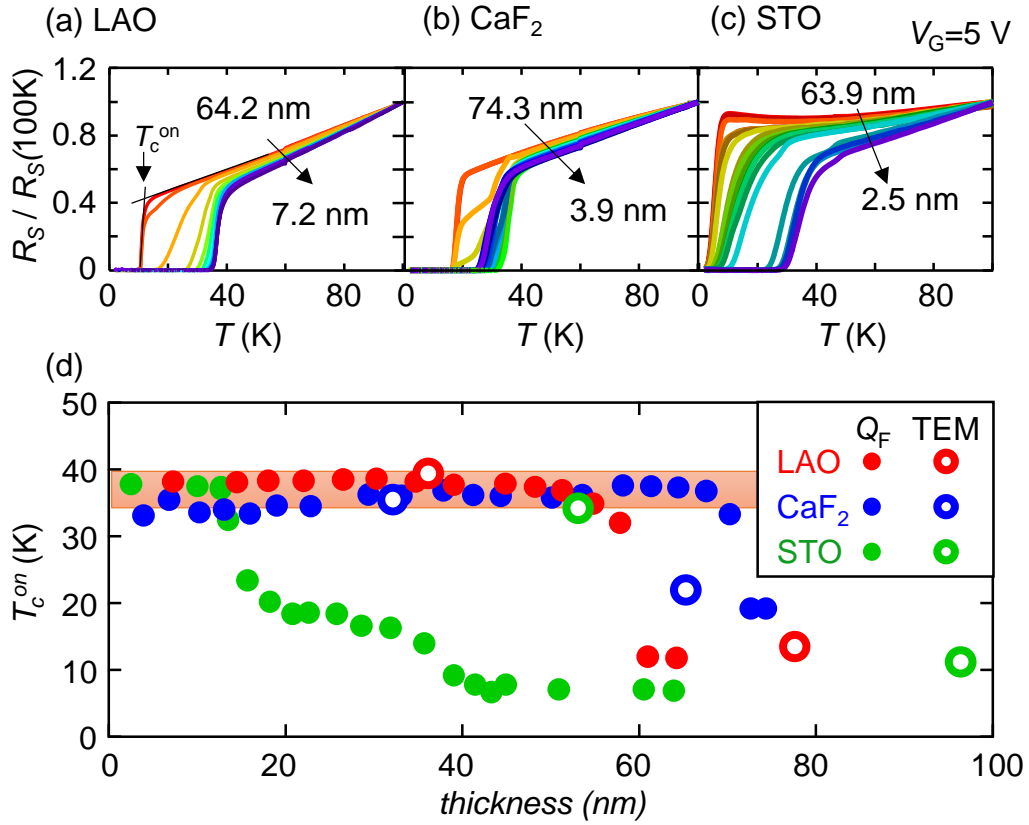


Figure 3 (a)-(c)  $T$  dependence of  $R_S$  normalized by  $R_S$  at 100 K,  $R_S(100K)$  for LAO, CaF<sub>2</sub> and STO samples, respectively, with the electrochemical etching for  $V_G = 5$  V. (d) Thickness dependences of  $T_c^{onset}$  for the three samples. Filled symbols correspond to the data shown in (a)-(c), where the thickness was estimated from  $Q_F$ . Open symbols correspond to other samples where the thickness after the etching was directly measured by the TEM measurement shown in Fig. 4.

The  $T_c$  enhancement on the thick samples was confirmed on other samples by TEM and XRD measurements. We made the etching experiments for other samples on LAO,  $\text{CaF}_2$  and STO substrates, and the etching was stopped after several cycles. All of the etched samples showed superconductivity at  $T_c$  above 34 K. The film thickness after the etching was directly obtained by TEM. The thickness dependences of  $T_c^{\text{onset}}$  for these samples were shown in Fig. 3 (d).  $\text{FeSe}_{0.8}\text{Te}_{0.2}$  films on all of LAO,  $\text{CaF}_2$  and STO substrates show  $T_c$  enhancement on films with a thickness above 30 nm. As shown in Fig. 4 (a), (b), and S. Fig. 1 (a), (e) in the supplementary information, all films have smooth interface between the substrate and the film, and a clear periodicity of atomic arrays are observed. The bright area at the interface probably indicates Se diffusion from the film into the substrate.<sup>29,30</sup> The clear periodicity is kept to the surface and no additional layer was found on the film on LAO substrate, as shown in Fig. 4 (a). On  $\text{CaF}_2$  and STO substrate, a disordered  $\text{FeO}_x$  layer was found on the ordered area with the clear periodicity. The  $T_c$  enhancement probably occurred in the ordered area. X-ray diffraction patterns before and after the etching indicate that the peak position was unchanged and no new peak was found after the etching, as shown in Fig. 4 (c), except for the decrease of the peak intensity. In addition, the FWHM of the rocking curve for the (001) peak was unchanged, as shown in Fig. 4 (d). These XRD data indicates that no new phase was created in the film by the etching. An electrochemical reaction did not occur at the bulk region of the film, but rather takes place only at the surface of the film.

Figure 4

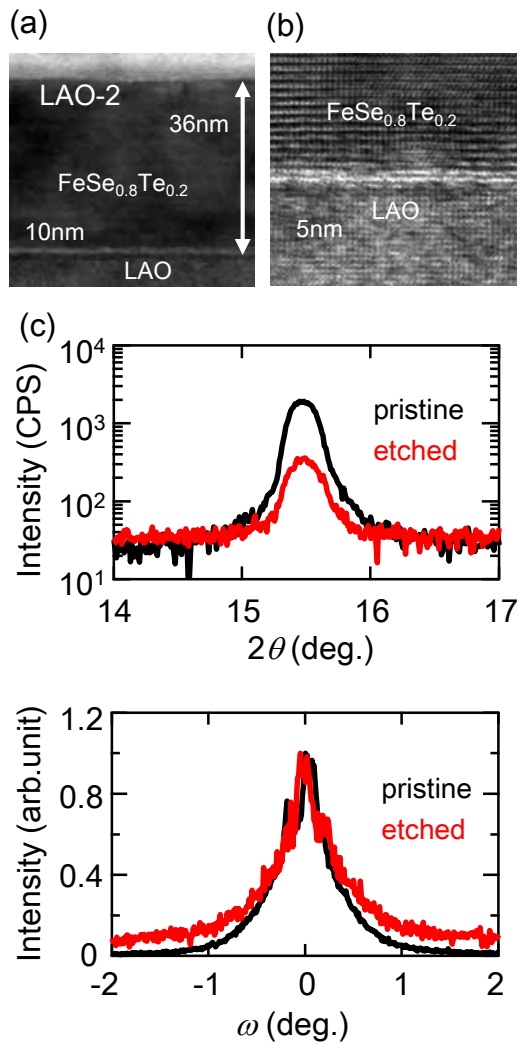


Figure 4 Physical properties of an identical sample on the LAO substrate before (pristine) and after (etched) electrochemical etching. (a), (b) TEM images for the etched sample (c) XRD diffraction patterns (d) Rocking curves for the (001) diffraction peak of the film. The intensity was normalized at  $\omega = 0$ .

We also examined thickness dependence of  $T_c$  for FeSe films on LAO and STO substrates. As shown in S. Fig. 2(a) and (b), these films showed the  $T_c$  enhancement up to 30 or 40 K by etching the samples. Films on STO substrate showed the  $T_c$  enhancement with thicknesses only below 12 nm. This coincides with the previous reports.<sup>16</sup> In contrast, a film on the LAO substrate showed the  $T_c$  enhancement with a thickness of 30 nm, which is similar to those on FeSe<sub>0.8</sub>Te<sub>0.2</sub> films. It is also noted that several FeSe<sub>0.8</sub>Te<sub>0.2</sub> samples on the CaF<sub>2</sub> and STO substrates showed the  $T_c$  enhancement above 37 K with the thickness only below 10 nm. The different critical thicknesses for FeSe and FeSe<sub>0.8</sub>Te<sub>0.2</sub> films on various substrates are probably due to the difference in the film homogeneity. As shown in S. Fig. 1(a) and (e) in the supplementary information, there is a disordered area in the FeSe<sub>0.8</sub>Te<sub>0.2</sub> film on STO. In addition, disordered Fe (or FeO<sub>x</sub>) layer was also observed on the top of the FeSe<sub>0.8</sub>Te<sub>0.2</sub> films on the CaF<sub>2</sub> and STO substrates. These TEM images indicate that the film quality depends on the substrates, and the FeSe<sub>0.8</sub>Te<sub>0.2</sub> film on the LAO substrate has the best quality. We consider that a good film quality in an entire film is necessary for the  $T_c$  enhancement on a thick film. Although we did not carry out the TEM measurements for all of these samples, no  $T_c$  enhancement to 38 K on the thick film on some samples might be due to insufficient film homogeneity, especially around the surface.

Finally, we discuss the origin of the  $T_c$  enhancement. The origin of the  $T_c$  enhancement has been reported to be due to a charge accumulation on the surface of the FeSe.<sup>15,16,18</sup> However, an electrochemically reacted layer on the surface may show a high  $T_c$ , since FeSe samples intercalated by alkali ions and/or organic molecules show  $T_c$  above 40 K.<sup>8,9</sup> In order to distinguish the electrostatic charge accumulation from the electrochemical reaction, we estimated the sheet resistance and the Hall coefficient of the surface layer. The resistance tensor,  $\rho$ , and the conductance tensor,  $\sigma$ , are represented by following equations,

$$\rho = \begin{pmatrix} R_S & -R_H B \\ R_H B & R_S \end{pmatrix},$$

$$\sigma = \rho^{-1} = \frac{1}{R_S^2 + R_H^2 B^2} \begin{pmatrix} R_S & R_H B \\ -R_H B & R_S \end{pmatrix} \sim \begin{pmatrix} 1/R_S & R_H B/R_S \\ -R_H B/R_S & 1/R_S \end{pmatrix},$$

where  $B$  is the applied magnetic field during the Hall measurement.  $\sigma$  of a sample for  $V_G = 5$  V is equal to the sum of  $\sigma$  of the sample for  $V_G = 0$  V and the surface conducting layer produced by  $V_G$  of 5 V. Therefore, the sheet resistance and the Hall coefficient of the surface conducting layer,  $R_S^{\text{surface}}$  and  $R_H^{\text{surface}}$ , follows these equations,

$$\frac{1}{R_{xx}(V_G = 5V)} = \frac{1}{R_{xx}(V_G = 0V)} + \frac{1}{R_{xx}^{\text{surface}}}$$

$$\frac{R_H(V_G = 5V)}{R_{xx}(V_G = 5V)} = \frac{R_H(V_G = 0V)}{R_{xx}(V_G = 0V)} + \frac{R_H^{\text{surface}}}{R_{xx}^{\text{surface}}}$$

As shown in Fig. 5 (b), (c) and (d), we examined the change in the sheet resistance and the Hall

coefficient once for the LAO sample (LAO-1, as shown in Fig. 2 (c)) and twice for the CaF<sub>2</sub> sample (CaF<sub>2</sub>-1 and CaF<sub>2</sub>-2. Data for CaF<sub>2</sub>-1 are shown in Fig. 2(d)). Figure 5 (a) shows the temperature dependence of  $R_S^{\text{surface}}$  normalized by the value at 90 K. The  $R_S$ - $T$  curves for the LAO and CaF<sub>2</sub> samples just before the last etching,  $R_S(\text{last})$ , are also plotted. All curves follow almost an identical curve. This indicates that all samples have an identical temperature dependence of the transport properties, such as the electron mobility and the scattering time. As shown in the inset of Fig. 5 (a),  $R_H$  was almost temperature independent and negative for all samples. The electron-type conduction is a common feature in previous reports on the  $T_c$  enhancement of FeSe,<sup>7,15-18</sup> and the vanish of the hole pocket on the Fermi level has been considered to be an origin of the  $T_c$  enhancement.<sup>7,15,16</sup> The observed Hall coefficient of 0.05 to 0.2 m<sup>2</sup>/C corresponds 4-17 electrons per one unit cell in two dimension ( 0.376 nm×0.376 nm). If such a high density carriers are electrostatically accumulated on the surface, electrons are strongly scattered at the surface, and the scattering time should change with changing the accumulated carrier density.<sup>31</sup> However, no such change was observed in the  $R$ - $T$  curve. In addition, as shown previously in Fig. 2 (c) and (d), the removal of  $V_G$  irreversibly changed  $R_S$ , suggesting another origin of a change in  $R_S$  than the electrostatic carrier doping. Therefore, another origin of carrier doping than electric field effect is likely responsible for the  $T_c$  enhancement.

Both the irreversible change in  $R_S$  with  $V_G$  and the identical electron mobility with carrier doping can be explained by assuming that the surface conducting layer is not formed by the electrostatic charge accumulation, but formed by the electrochemical reaction between FeSe and ionic liquid. We assume that the etching of the film and the formation of the surface conducting layer simultaneously occurred by applying  $V_G$  of 5 V. In addition, when  $V_G$  was removed, we assume that the surface conducting layer disappeared probably due to a decomposition or peeling off from the surface. Then, the abrupt decrease in the sheet conductance occurred by removing  $V$ . In addition, both the electron mobility and the volume charge carrier density would be identical in all of LAO-1, CaF<sub>2</sub>-1 and CaF<sub>2</sub>-2. This assumption was also supported by the change of the sheet conductance with the repetition of the etching on the LAO and CaF<sub>2</sub> samples, as shown in Fig. 5 (d). The sheet conductance at 50 K showed the reduction by removing  $V_G$ , and gradually increased by repeating the etching after the reduction. This is explained by an increase of the thickness of the surface conducting layer by the repetition of the etching. If the conductance of the surface conducting layer is larger than that of the bulk FeSe<sub>0.8</sub>Te<sub>0.2</sub> film at 50 K, the repetition of the etching increase the sheet conductance at low temperatures. As repeating the etching, ratio of the surface conducting layer to the total film thickness increased. Then, just before the film was totally removed, the surface conducting layer covers almost entire film. Therefore, the temperature dependences of the sheet resistance just before the last etching of both LAO and CaF<sub>2</sub> samples were also identical to that of the surface conducting layer, as shown in Fig. 5 (a).

In conclusion, the surface conducting layer with  $T_c$  of 38 K was commonly formed by the electrochemical etching of  $\text{FeSe}_{0.8}\text{Te}_{0.2}$  thin films on LAO,  $\text{CaF}_2$  and STO substrate. Since the thickness of the etched samples with  $T_c$  of 38 K is higher than 30 nm for all samples, the enhancement of  $T_c$  is not related to any interaction between the film and the substrate. In addition, the  $T_c$  enhancement was also observed on a FeSe thin film on LAO substrate with a thickness of around 30 nm. The surface conducting layer also showed almost the identical temperature dependence of the sheet resistance and the Hall coefficient. This suggests that the surface conducting layer is not formed by the electrostatic charge accumulation on the  $\text{FeSe}_{0.8}\text{Te}_{0.2}$  surface, but formed by the electrochemical reaction between  $\text{FeSe}_{0.8}\text{Te}_{0.2}$  and ionic liquid electrolyte. The Hall coefficient measurement showed that the surface conducting layer includes 4-17 electrons per one unit cell in two dimension with negative sign. From the TEM measurement, we can observe smooth interface between the substrate and the film and a clear periodicity of atomic arrays on the etched  $\text{FeSe}_{0.8}\text{Te}_{0.2}$  film on LAO substrate. These indicate that the formation of the surface conducting layer does not affect bulk region of the film, and the surface conducting layer completely disappeared by removing  $V_G$ . We consider that previous studies on the carrier doping on FeSe ultrathin film are classified to two groups; one is on  $T_c$  of around 40 K on a several-layer FeSe film, and another is on  $T_c$  above 65 K on a monolayer FeSe on STO. Our results indicate that the electrochemical doping on FeSe and  $\text{FeSe}_{0.8}\text{Te}_{0.2}$  can form the superconducting layer with  $T_c$  of around 40 K, and no interface interaction is necessary for the  $T_c$  enhancement to 40 K. But we think that the interface between FeSe and STO is probably essential for the  $T_c$  enhancement above 65 K. We believe that the monolayer FeSe with  $T_c$  above 65 K will be prepared by further study on the electrochemical etching of FeSe.

### **Acknowledgement**

This work was partly supported by JSPS KAKENHI (Grant Numbers 25708039, 25220604) and CREST-JST.

Figure 5

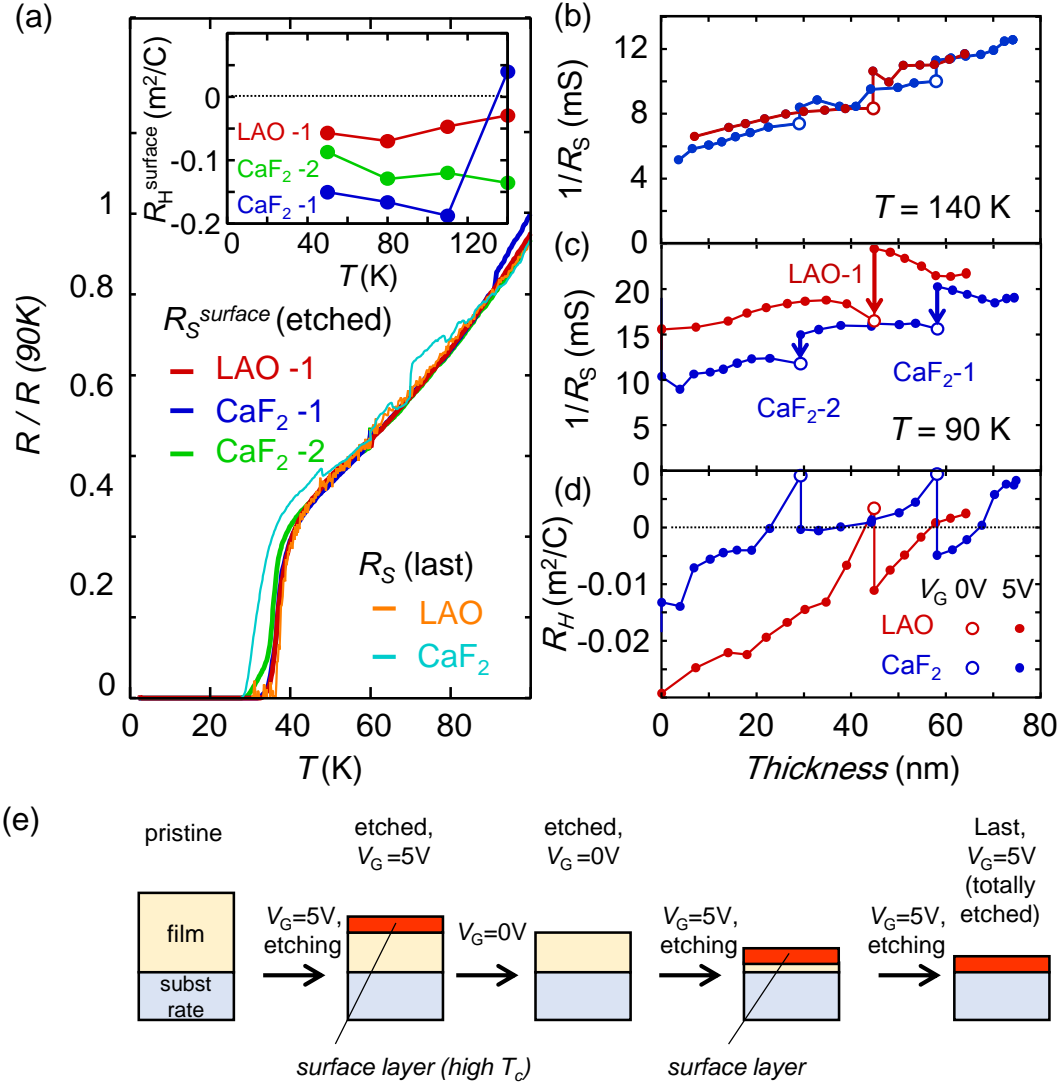


Figure 5 (a) The  $T$  dependence of the sheet resistance of the surface conducting layer ( $R_S^{\text{surface}}$ ) normalized by the value at 90 K.  $R_S^{\text{surface}}$  was estimated from a change of sheet conductance between  $V_G$  of 5 V and 0 V. Data for LAO-1, CaF<sub>2</sub>-1 and CaF<sub>2</sub>-2 are shown. The  $R_S$ - $T$  curves just before the last etching for the LAO and CaF<sub>2</sub> samples were also plotted. The inset shows  $R_H$  of the surface conducting layer for the LAO-1, CaF<sub>2</sub>-1 and CaF<sub>2</sub>-2 samples as a function of temperature. (b),(c), (d)  $1/R_S$  at 140 K and 90 K, and  $R_H$  at 50 K, respectively, as a function of the film thickness for the LAO and CaF<sub>2</sub> samples.  $V_G$  was changed from 5 V to 0 V once and twice during the etching for the LAO and CaF<sub>2</sub> samples, respectively. (e) Schematic picture during etching. Surface layer was formed during the etching and disappeared by removing the gate bias.

## REFERENCES

- <sup>1</sup> F.-C. Hsu, J.-Y. Luo, K.-W. Yeh, T.-K. Chen, T.-W. Huang, P.M. Wu, Y.-C. Lee, Y.-L. Huang, Y.-Y. Chu, D.-C. Yan, and M.-K. Wu, *Proc. Natl. Acad. Sci.* **105**, 14262 (2008).
- <sup>2</sup> J.-F. Ge, Z.-L. Liu, C. Liu, C.-L. Gao, D. Qian, Q.-K. Xue, Y. Liu, and J.-F. Jia, *Nat. Mater.* **14**, 285 (2015).
- <sup>3</sup> Y. Sun, W. Zhang, Y. Xing, F. Li, Y. Zhao, Z. Xia, L. Wang, X. Ma, Q.-K. Xue, and J. Wang, *Sci. Rep.* **4**, 6040 (2014).
- <sup>4</sup> S. He, J. He, W. Zhang, L. Zhao, D. Liu, X. Liu, D. Mou, Y.-B. Ou, Q.-Y. Wang, Z. Li, L. Wang, Y. Peng, Y. Liu, C. Chen, L. Yu, G. Liu, X. Dong, J. Zhang, C. Chen, Z. Xu, X. Chen, X. Ma, Q. Xue, and X.J. Zhou, *Nat. Mater.* **12**, 605 (2013).
- <sup>5</sup> W. Qing-Yan, L. Zhi, Z. Wen-Hao, Z. Zuo-Cheng, Z. Jin-Song, L. Wei, D. Hao, O. Yun-Bo, Deng Peng, C. Kai, W. Jing, S. Can-Li, H. Ke, J. Jin-Feng, J. Shuai-Hua, W. Ya-Yu, W. Li-Li, C. Xi, Ma Xu-Cun, and X. Qi-Kun, *Chin. Phys. Lett.* **29**, 037402 (2012).
- <sup>6</sup> S. Tan, Y. Zhang, M. Xia, Z. Ye, F. Chen, X. Xie, R. Peng, D. Xu, Q. Fan, H. Xu, J. Jiang, T. Zhang, X. Lai, T. Xiang, J. Hu, B. Xie, and D. Feng, *Nat. Mater.* **12**, 634 (2013).
- <sup>7</sup> Y. Miyata, K. Nakayama, K. Sugawara, T. Sato, and T. Takahashi, *Nat. Mater.* **14**, 775 (2015).
- <sup>8</sup> M. Burrard-Lucas, D.G. Free, S.J. Sedlmaier, J.D. Wright, S.J. Cassidy, Y. Hara, A.J. Corkett, T. Lancaster, P.J. Baker, S.J. Blundell, and S.J. Clarke, *Nat. Mater.* **12**, 15 (2013).
- <sup>9</sup> T. Hatakeda, T. Noji, K. Sato, T. Kawamata, M. Kato, and Y. Koike, *J. Phys. Soc. Jpn.* **85**, 103702 (2016).
- <sup>10</sup> A.F. Wang, J.J. Ying, Y.J. Yan, R.H. Liu, X.G. Luo, Z.Y. Li, X.F. Wang, M. Zhang, G.J. Ye, P. Cheng, Z.J. Xiang, and X.H. Chen, *Phys. Rev. B* **83**, 060512 (2011).
- <sup>11</sup> Y. Zhang, L.X. Yang, M. Xu, Z.R. Ye, F. Chen, C. He, H.C. Xu, J. Jiang, B.P. Xie, J.J. Ying, X.F. Wang, X.H. Chen, J.P. Hu, M. Matsunami, S. Kimura, and D.L. Feng, *Nat. Mater.* **10**, 273 (2011).
- <sup>12</sup> T.P. Ying, X.L. Chen, G. Wang, S.F. Jin, T.T. Zhou, X.F. Lai, H. Zhang, and W.Y. Wang, *Sci. Rep.* **2**, 426 (2012).
- <sup>13</sup> A. Krzton-Maziopa, E.V. Pomjakushina, V.Y. Pomjakushin, F. von Rohr, A. Schilling, and K. Conder, *J. Phys. Condens. Matter* **24**, 382202 (2012).
- <sup>14</sup> X.F. Lu, N.Z. Wang, H. Wu, Y.P. Wu, D. Zhao, X.Z. Zeng, X.G. Luo, T. Wu, W. Bao, G.H. Zhang, F.Q. Huang, Q.Z. Huang, and X.H. Chen, *Nat. Mater.* **14**, 325 (2015).
- <sup>15</sup> B. Lei, J.H. Cui, Z.J. Xiang, C. Shang, N.Z. Wang, G.J. Ye, X.G. Luo, T. Wu, Z. Sun, and X.H. Chen, *Phys. Rev. Lett.* **116**, 077002 (2016).
- <sup>16</sup> J. Shioagai, Y. Ito, T. Mitsuhashi, T. Nojima, and A. Tsukazaki, *Nat. Phys.* **12**, 42 (2016).
- <sup>17</sup> K. Hanzawa, H. Sato, H. Hiramatsu, T. Kamiya, and H. Hosono, *IEEE Trans. Appl. Supercond.* **27**, 1 (2017).

- <sup>18</sup> K. Hanzawa, H. Sato, H. Hiramatsu, T. Kamiya, and H. Hosono, *Proc. Natl. Acad. Sci.* **113**, 3986 (2016).
- <sup>19</sup> J. Shiogai, T. Miyakawa, Y. Ito, T. Nojima, and A. Tsukazaki, *Phys. Rev. B* **95**, 115101 (2017).
- <sup>20</sup> K. Ueno, S. Nakamura, H. Shimotani, A. Ohtomo, N. Kimura, T. Nojima, H. Aoki, Y. Iwasa, and M. Kawasaki, *Nat Mater* **7**, 855 (2008).
- <sup>21</sup> H. Yuan, H. Shimotani, A. Tsukazaki, A. Ohtomo, M. Kawasaki, and Y. Iwasa, *Adv. Funct. Mater.* **19**, 1046 (2009).
- <sup>22</sup> K. Ueno, H. Shimotani, H. Yuan, J. Ye, M. Kawasaki, and Y. Iwasa, *J. Phys. Soc. Jpn.* **83**, 032001 (2014).
- <sup>23</sup> Y. Imai, Y. Sawada, F. Nabeshima, and A. Maeda, *Proc. Natl. Acad. Sci. U. S. A.* **112**, 1937 (2015).
- <sup>24</sup> Y. Imai, Y. Sawada, F. Nabeshima, D. Asami, M. Kawai, and A. Maeda, *Sci. Rep.* **7**, srep46653 (2017).
- <sup>25</sup> I. Tsukada, M. Hanawa, T. Akiike, F. Nabeshima, Y. Imai, A. Ichinose, S. Komiya, T. Hikage, T. Kawaguchi, H. Ikuta, and A. Maeda, *Appl. Phys. Express* **4**, 053101 (2011).
- <sup>26</sup> F. Nabeshima, Y. Imai, M. Hanawa, I. Tsukada, and A. Maeda, *Appl. Phys. Lett.* **103**, 172602 (2013).
- <sup>27</sup> Y. Imai, R. Tanaka, T. Akiike, M. Hanawa, I. Tsukada, and A. Maeda, *Jpn. J. Appl. Phys.* **49**, 023101 (2010).
- <sup>28</sup> Y. Imai, T. Akiike, M. Hanawa, I. Tsukada, A. Ichinose, A. Maeda, T. Hikage, T. Kawaguchi, and H. Ikuta, *Appl. Phys. Express* **3**, 043102 (2010).
- <sup>29</sup> A. Ichinose, F. Nabeshima, I. Tsukada, M. Hanawa, S. Komiya, T. Akiike, Y. Imai, and A. Maeda, *Supercond. Sci. Technol.* **26**, 075002 (2013).
- <sup>30</sup> I. Tsukada, A. Ichinose, F. Nabeshima, Y. Imai, and A. Maeda, *AIP Adv.* **6**, 095314 (2016).
- <sup>31</sup> Y. Sato, K. Doi, Y. Katayama, and K. Ueno, *Jpn. J. Appl. Phys.* **56**, 051101 (2017).

## Supplementary Information

### Superconductivity at 38 K in an electrochemical interface between ionic liquid and Fe(Se<sub>0.8</sub>Te<sub>0.2</sub>) on various substrates

Shunsuke Kouno,<sup>1</sup> Yohei Sato,<sup>1</sup> Yumiko Katayama,<sup>1</sup> Ataru Ichinose,<sup>2</sup> Daisuke Asami,<sup>1</sup> Fuyuki Nabeshima,<sup>1</sup> Yoshinori Imai,<sup>3</sup> Atsutaka Maeda,<sup>1</sup> and Kazunori Ueno<sup>1\*</sup>

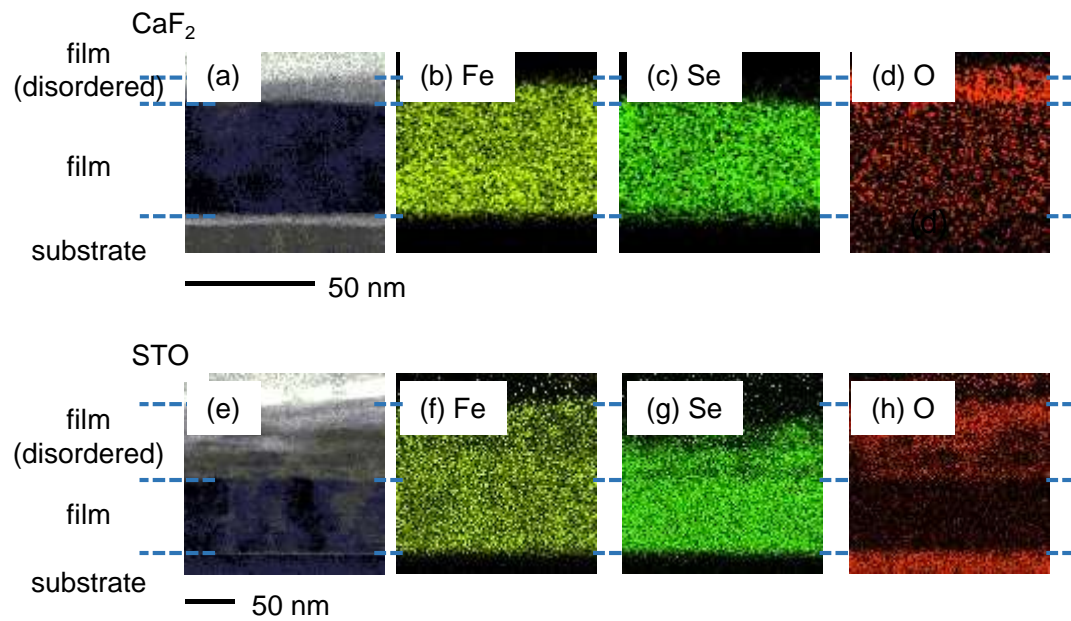
<sup>1</sup>*Department of Basic Science, University of Tokyo, Meguro, Tokyo 115-8902, Japan*

<sup>2</sup>*Central Research Institute of Electric Power Industry, Yokosuka, Kanagawa 240-0196, Japan*

<sup>3</sup>*Department of Physics, Tohoku University, Sendai 980-8578, Japan*

#### TEM images after etching for samples on CaF<sub>2</sub> and SrTiO<sub>3</sub>

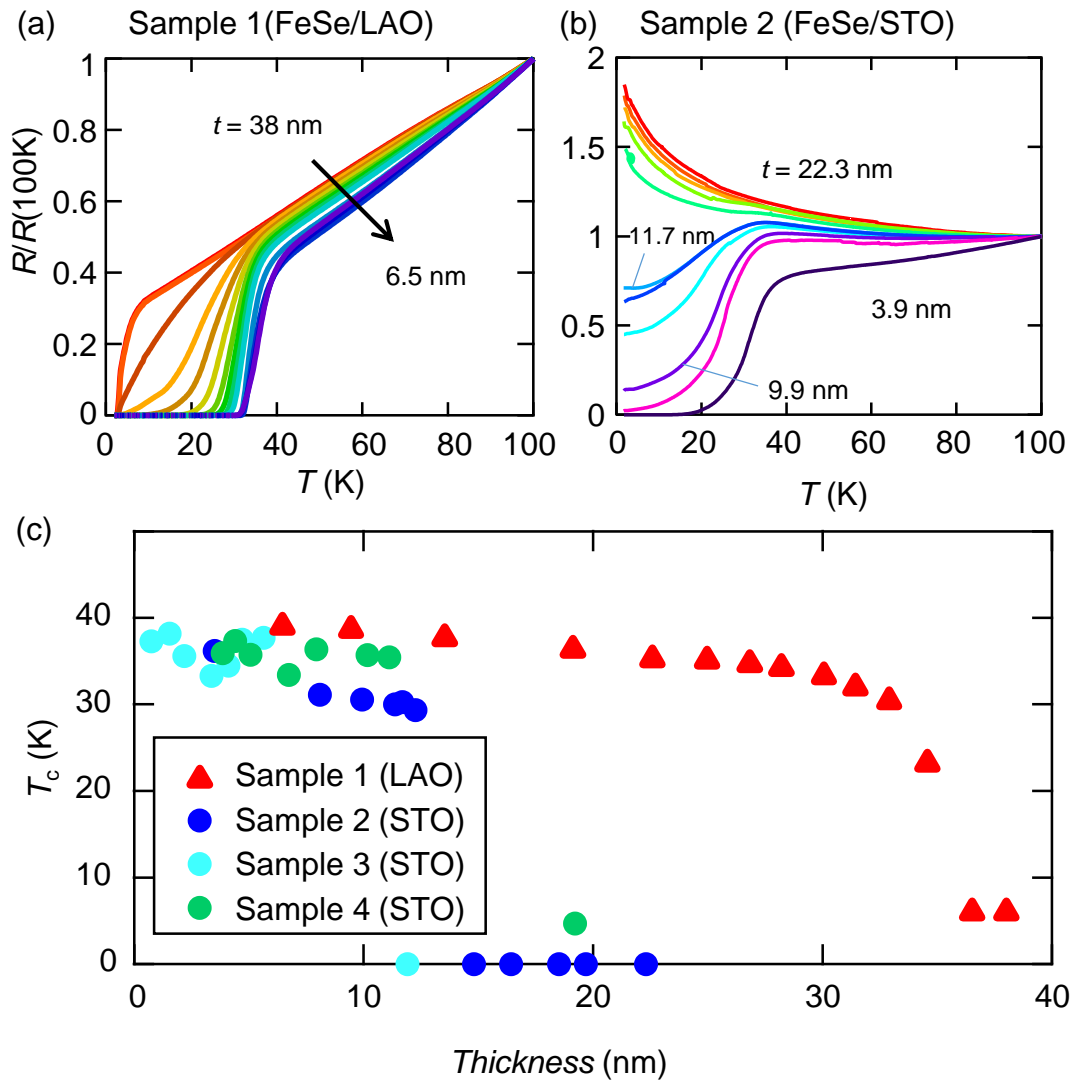
Scanning TEM experiments were performed on FeSe<sub>0.8</sub>Te<sub>0.2</sub> films on CaF<sub>2</sub> and STO substrates.  $T_c$  was changed from 22.0 K to 35.5 K for the film on the CaF<sub>2</sub> substrate and 11.2 K to 34.K for the film on the STO substrate after several cycles of the etching. Topographic images for both films include a bright area with a thickness of several atomic layers at the interface between the substrate and the film, probably indicating Se diffusion from the film into the substrate. In addition, both films include a bright, disordered area on the top of a dark area with a clear periodic atomic arrays. Since O and Fe atoms are observed but Se atoms are not observed in the disordered area, this area corresponds to the oxidized Fe (FeO<sub>x</sub>) layer. In addition, there are no FeO<sub>x</sub> peaks from the  $2\theta$ - $\theta$  measurement by the XRD before and after the etching, the FeO<sub>x</sub> is a polycrystal or an amorphous. The FeO<sub>x</sub> layer possibly originates from chemical reaction between air and a residual Fe layer after the electrochemical etching of FeSe. We estimated a film thickness from the dark, well-crystallized FeSe area and plotted in Fig. 3 in the manuscript.



S. Figure 1 Topographic image of scanning TEM and EDX mapping images of Fe, Se and O. (a)-(d) correspond to  $\text{FeSe}_{0.8}\text{Te}_{0.2}$  film on  $\text{CaF}_2$  substrate. (e)-(h) correspond to  $\text{FeSe}_{0.8}\text{Te}_{0.2}$  film on  $\text{SrTiO}_3$  substrate.

## Thickness dependence of superconducting critical temperature for FeSe thin films on LAO and STO substrates

One FeSe film and three FeSe films were fabricated on LAO and STO substrates, respectively. The films were etched for  $V_G$  of 5 V and the temperature dependence of the resistance was measured after the each etching cycle. Temperature dependence of the resistance is shown in S. Fig. 2(a) and (b). Critical temperature rapidly increased for the film on the LAO substrate. In contrast, the film on the STO substrate showed a  $T_c$  increase with a thickness of around 10 nm. S. Figure 2(c) shows the thickness dependence of  $T_c^{\text{onset}}$  for all FeSe samples.



S. Figure 2 (a), (b) Temperature dependence of sheet resistance  $R$  normalized by  $R$  at 100 K with various thicknesses  $t$ . (c) Thickness dependence of superconducting critical temperature  $T_c^{\text{onset}}$  for FeSe samples on LAO and STO substrates.

